Boride Nanoparticles

DOI: 10.1002/anie.201006810

A General Solution Route toward Metal Boride Nanocrystals**

David Portehault, Sarala Devi, Patricia Beaunier, Christel Gervais, Cristina Giordano, Clément Sanchez, and Markus Antonietti*

Metal–boron alloys contain a boron covalent framework providing typical high chemical, mechanical, and thermal stability, which allows important applications, for example, for diborides (NbB_2) and hexaborides (CaB_6) as refractory materials.[1] New properties also arise from alloying; a prime example is the superconductivity of magnesium diboride, which exhibits the highest critical temperature (39 K) among classical superconductors.[2] Hexaborides are also relevant because of their field emission properties[3] and their potential for thermoelectricity (CeB_6).[4] Moreover, transition-metal borides are drawing attention as efficient (de)hydrogenation catalysts that can accelerate, for instance, emission of hydrogen from ammonia–borane or borohydrides within energy-harnessing devices based on hydrogen technology.[5] Applications in hyperthermia, information storage, thermoelectricity, and catalysis would benefit from scaling down to the nanometer range, which could bring, as for all nanomaterials, modified, enhanced, and even novel properties that arise from the finite particle size. To date, only a few nanostructured borides have been reported. This paucity arises mainly because M–B systems are typically synthesized at high temperatures above 1100 °C.[6] Nanoscale materials have been obtained at lower temperatures (25–100 °C), but at the expense of crystallinity and stability, and such approaches yield pyrophoric compounds without applicability.[7] The scarce reported procedures for nanostructured crystalline systems rely on physical[5,8] or chemical methods,[9] and none of them is demonstrated to be generally applicable to the wide and rich family of borides. Moreover, the majority of crystalline metal borides has not yet been approached at the nanoscale, such as hard (HfB_2) or ultrahard (MoB_4) materials, catalysts, and ferromagnetic compounds (FeB). The development of a reliable, versatile, and general synthesis procedure towards such systems is therefore still eagerly demanded.

One requirement to obtain such nanostructures is the use of relatively mild temperatures, which are still high enough to trigger crystallization but low enough to avoid excessive grain growth, ideally in the range 500–900 °C. Then, development of a solution route instead of standard solid-state reactions may contribute to full kinetic accessibility of the reaction space, which includes control of nanocrystal size and shape.[10] Because of the thermal instability of organic solvents in such conditions, we turned to inorganic molten salts, which are readily available and safe to apply at the targeted temperatures.

Herein we present the use of such salt melts for the first general synthesis of metal boride nanocrystals. The method is based on a one-pot ionothermal process which is simple and relies on medium temperature, atmospheric pressure, and environmentally friendly solvents. Applicability to a wide range of compounds, formation of novel nanostructures, and control over the nanocrystal size and the material texture are demonstrated. Processing of the nanoparticles within borosilicate glass-ceramic composites and tuning of the material conductivity are finally described.

Solid metal chlorides as metal precursors and sodium borohydride as the boron source and reductant were selected in order to avoid oxygen- and moisture-containing species, which could yield side reactions.[11] The eutectic LiCl/KCl (45:55 wt.) mixture was chosen as a cheap, sustainable, water-soluble and low-melting-point solvent (355 °C) to trigger reactions in the liquid state.[12] The powders were mixed at room temperature and heated under argon flow. After cooling and solvent removal by water washing, black powders were recovered. Various systems were examined to assess the relevance of the procedure for hexaborides (CaB_6, CeB_6), tetraborides (MoB_4), diborides (NbB_2, HfB_2), and lower borides (FeB, Mn_2B). We focus below on NbB_2 and CaB_6 as proofs of concept, then we assess other technologically relevant compounds to demonstrate the generality of the approach.

XRD patterns (see the Supporting Information) indicate that diboride NbB_2 and hexaboride CaB_6 are obtained at 900 and 800 °C, respectively, as pure crystalline phases when an excess of boron precursor is used for NbB_2 (initial Nb/B $\leq$ 1:4) or a stoichiometric amount for CaB_6 (initial Ca/B $\leq$ 1:6). Refined cell parameters for NbB_2 are $a = 3.096$ Å and $c = 3.298$ Å, a clear downwards and upwards shift in comparison to stoichiometric bulk NbB_2, thus indicating a boron-rich

[*] Dr. D. Portehault, Dr. S. Devi, Dr. C. Giordano, Prof. M. Antonietti
Max-Planck-Institute of Colloids and Interfaces
Department of Colloid Chemistry
Campus Golm, 14424 Potsdam (Germany)
Fax: (+49) 331-567-9502
E-mail: david.portehault@upmc.fr
Homepage: http://www.labos.upmc.fr/lcmcp/
P. Beaunier
Laboratoire de Réactivité de Surface
UPMC Univ Paris 06, CNRS, UMR 7609
75252 Paris Cedex 05 (France)
Dr. C. Gervais, Prof. C. Sanchez
Chimie de la Matière Condensée de Paris
UPMC Univ Paris 06, CNRS, UMR 7574, Collège de France
11 place Marcelin Berthelot, 75231 Paris Cedex 05 (France)

[**] We acknowledge financial funding from the Max Planck Institute—CNRS Post-Doctoral Program for Nanomaterials.

Supporting information for this article, including experimental procedures, XRD patterns, FTIR and NMR spectra, and SEM and TEM images, is available on the WWW under http://dx.doi.org/10.1002/anie.201006810.

WILEY ONLINE LIBRARY © 2011 Wiley-VCH Verlag GmbH & Co. KGaA, Weinheim

compound with B/Nb ≈ 2.1.[13] The refined cell parameter for cubic CaB_6 is 4.144 Å, in agreement with the literature.[8a] Broadened reflections that result when the initial amount of boron is increased highlight a strong decrease of the crystallite size from 7 (Nb/B = 1:4) to 3 nm (1:8) for NbB_2 and 16 (Ca/B = 1:6) to 10 nm (1:12) for CaB_6 according to the Scherrer formula. Brunauer–Emmett–Teller analysis of the N_2 sorption isotherms provides specific surface area values of 25 (Nb/B = 1:4) and 120 $m^2 g^{-1}$ (1:8) for NbB_2, in agreement with the decreased crystallite size. CaB_6 is obtained with 10 $m^2 g^{-1}$ (Ca/B = 1:6) and 80 $m^2 g^{-1}$ (1:12). To our knowledge, such high values were never reported for metal borides (e.g. 16 $m^2 g^{-1}$ for NbB_2[9e]) and, taking into account the high densities, can compare favorably with common high-surface-area materials used especially for catalysis.[14] Scanning electron microscopy (see the Supporting Information) and transmission electron microscopy (TEM, see Figure 1 and the Supporting Information) indicate that samples are homogeneously composed of nanoparticles embedded in an amorphous matrix of 2 nm thickness. NbB_2 nanocrystals exhibit diameters of approximately 10 and 5 nm for initial ratios of Nb/B = 1:4 and 1:8, respectively, in agreement with XRD. These values are one order of magnitude lower than those previously reported.[15] The smallest CaB_6 nanoparticles obtained to date, with 10 nm diameter, are also evidenced (see the Supporting Information).[8a] For all of the investigated metal–boron systems, the nanoparticles are single crystals. XRD and electron microscopy demonstrate that size tuning can be effectively achieved by adjusting the boron-source concentration. Although in-depth study of the reaction pathway will require further work, the decrease of the particle size that results when the concentration of one reactant is increased can be easily comprehended in the framework of classical crystal growth theory as a nucleation-driven phenomenon. Indeed, a higher precursor concentration leads to a higher nucleation rate, a higher number of nuclei for the same amount of material, and thus to smaller nanoparticles.[16]

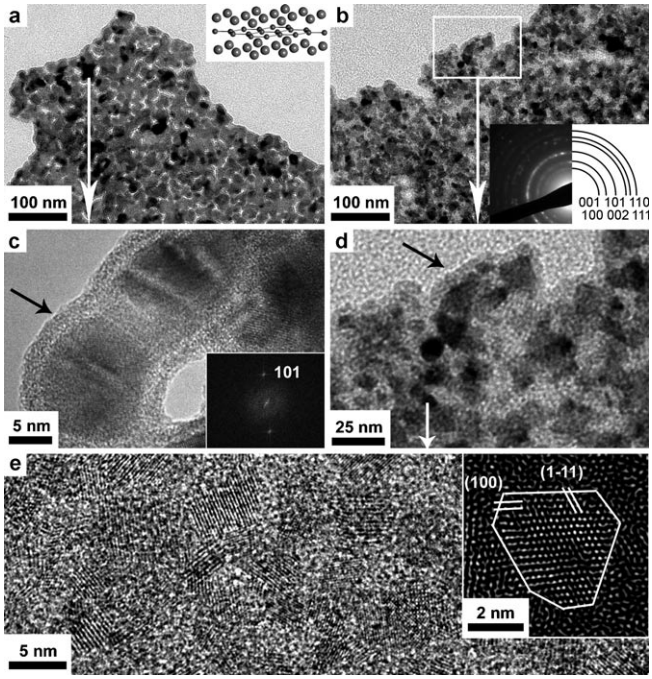

Figure 1. TEM pictures of niobium diboride nanocrystals obtained at 900 °C with $NbCl_5/NaBH_4$ = 1:4 (a, c) and 1:8 (b, d, e). Corresponding SAED pattern (c) and Fourier filtered HRTEM zoom (e) are shown as insets. The black arrows (c, d) highlight an amorphous matrix embedding the particles.

Elemental analysis of a NbB_2 sample for initial Nb/B = 1:8 yields a Nb/B ratio of approximately 0.14 (1:7) (Ca/B = 0.10 (1:10) for CaB_6 obtained for initial Ca/B = 1:12) and highlights an excess of boron in the material, thus indicating that the amorphous component observed by TEM is mainly composed of boron. The Nb, B, and O contents for initial Nb/B = 1:8 lead to $O/B_{am} = 0.7$ within the amorphous phase, which suggests that this compound is made of partially oxidized amorphous boron. This hypothesis is confirmed by Fourier transformed infrared (FTIR) spectra, which exhibit typical bands of B–O stretching modes at 1195, 1350, and 1450 cm^{-1} (see the Supporting Information),[17] while no Nb–O band is observed.[18] Moreover, the ^{11}B solid-state magic-angle spinning NMR spectrum (see the Supporting Information) gives clear evidence of BO_4 groups at approximately δ = 0 ppm, while a broad signal between δ = 25 and −40 ppm corresponds most probably to BB_x groups in the amorphous phase and crystalline NbB_2. To provide further evidence of the nature of this component, selective etching was performed in a hydrogen peroxide solution, resulting in the dissolution of the nanoparticles while the amorphous matrix was maintained (see the Supporting Information).[19] Comparison of the energy-dispersive X-ray analysis spectra before and after leaching shows that this matrix contains solely boron and oxygen, in agreement with elemental analysis and FTIR and NMR spectral data for the initial sample. These different techniques indicate that the matrix is made of partially oxidized amorphous boron. Attempts to dissolve this compound selectively were unsuccessful to date because of the known higher chemical inertness of amorphous oxidized boron versus crystalline metal borides.[19] The matrix could, however, provide interesting benefits, for example, for thermoelectrics by decreasing the thermal conductivity of boride composites.[20] It is also important to note for further evaluation of the properties that dissolution of the nanoparticles while the amorphous part is maintained shows that the nanocrystal surface is accessible to potentially reactive solutes. This point is of premium importance to evaluate the catalytic and electrochemical properties of the as-obtained metal boride nanocrystals.

Other technologically relevant binary borides were assessed to demonstrate the generality of the process. Firstly, hafnium diboride was obtained as an isomorph of niobium diboride (Figure 2a) with nanoparticles of ca. 50 nm. To our knowledge, this is the first report on HfB_2 particles in the nanometer range.[21] HfB_2 is an ultra-high-temperature ceramic with high mechanical strength and thermal and electrical conductivity, which is currently investigated as a wear-resistant coating for vehicles and as a diffusion barrier in microchips. All these applications could strongly benefit from the downscaling demonstrated herein. Secondly, cerium

 © 2011 Wiley-VCH Verlag GmbH & Co. KGaA, Weinheim

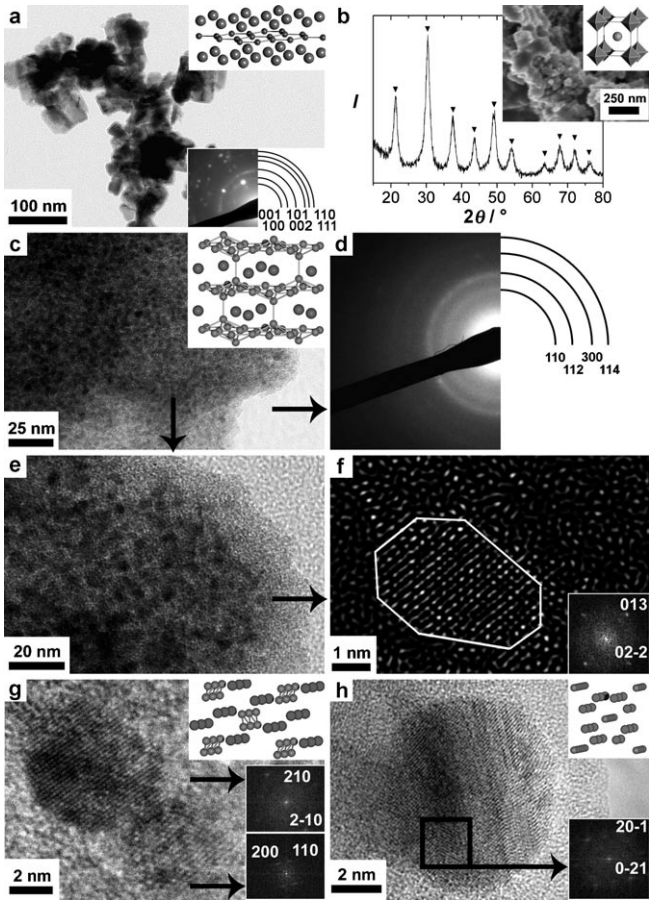

Figure 2. a) TEM picture and corresponding SAED pattern of HfB_2 nanocrystals. b) XRD pattern and SEM image of CeB_6 nanoparticles. c,e) TEM pictures, d) corresponding SAED pattern, and f) Fourier filtered HRTEM image of MoB_4 nanoparticles. HRTEM picture and corresponding Fourier transforms of g) FeB nanoparticles and h) a Mn_2B nanoparticle. Detailed synthesis parameters are given in the Supporting Information.

hexaboride CeB_6 was made as small nanoparticles of 8 nm diameter according to XRD and SEM (Figure 2b). This size is again one order of magnitude smaller than previously reported data.[8b,9d,f] The design of nanostructured CeB_6 and other rare-earth hexaborides could be relevant to the increase of efficiency in thermoelectrics and information storage.[4] Ultrahard materials can also be fabricated by the ionothermal process. Indeed, nanostructured MoB_4 was synthesized for the first time as a crystalline compound with nanoparticles of 4 nm diameter (Figure 2c–f). The SAED pattern and the HRTEM image could only be satisfactorily indexed along with the typical WB_4 crystal structure, which was recently suggested to be metastable.[22] This structure may originate from the relatively low temperatures used during the ionothermal process that enables the formation and isolation of non-equilibrium structures, potentially suggesting the possibility of synthesizing novel compounds. The synthesis of crystalline borides from the first transition series was exemplified by making the monoboride FeB (Figure 2g) and the lower boride Mn_2B (Figure 2h). These two examples are the first reported cases of FeB and of Mn_xB_y nanoscale systems. In contrast to their pyrophoric amorphous counterparts,[7a] these materials are stable upon air exposure and are expected to exhibit interesting magnetic and catalytic properties.[8c] Occurrence of different stoichiometries in borides of the first transition series is a complex issue. Especially, Mn_2B is obtained with by-product MnB, as evidenced by XRD. The question of multiphase occurrence in these systems will be addressed in further studies.

To evaluate the impact of downscaling on the properties and to analyze the potential of the as-prepared materials, conductivity measurements were performed by electrochemical impedance spectroscopy on pressed pellets. NbB_2 is a good representative of diborides as highly conductive bulk metals.[23] The conductivity of the NbB_2 samples obtained for Nb/B = 1:4 and 1:8 reaches 60% and 5%, respectively, of the value for a commercial bulk compound. The material composed of nanoparticles of 10 nm diameter, in spite of the amorphous side product, still exhibits excellent transport properties, while further decrease of the particle size causes a drop of the conductivity, which is likely related to grain boundary effects and the higher amount of amorphous boron phase. A similar behavior is observed with CaB_6, which belongs to the semimetals.[24]

Although the boron oxide layer can reduce the electrical conductivity of these systems, it can also be beneficial for processing the material. For instance, it acts as a functionalized buffer layer for incorporation of the particles into borosilicate glasses. We adapted a typical sol–gel process involving acidic catalysis of tetraethylorthosilicate condensation in the presence of NbB_2 nanocrystals. After drying the gels and calcination at 400 °C, NbB_2 is still observed by XRD, while FTIR spectra (see the Supporting Information) highlight a strengthening of B–O bands and the appearance of a characteristic B-O-Si band at approximately 650 cm^{-1}, which accounts for the formation of a borosilicate–NbB_2 glass-ceramic composite. Concentrations of NbB_2 nanocrystals up to 20 wt.% are attained. This approach demonstrates the possibility of processing the metal boride nanoparticles into glass pieces and layers.

In summary, we developed the first general route towards nanocrystals of metal borides. This ionothermal process enables the environmentally friendly one-pot synthesis at relatively low temperature and atmospheric pressure of various compounds, most of them being achieved at the nanoscale for the first time. The use of mild conditions enables easy adjustment of the particle size and the material texture. Indeed, various structures of metal borides can be fabricated, ranging from extended 3D (MB_6, MB_4), 2D (MB_2), and 1D (MB) boron frameworks to cluster-like compounds (M_2B). We are now embarking on detailed studies of the mechanistic aspects of the synthesis as well as of the properties of these new materials. Together with the ability to process the compounds into composites, the procedure displays in our opinion unprecedented versatility and enables us to address a wide range of novel functional materials.

Received: October 29, 2010
Revised: December 13, 2010
Published online: February 25, 2011

 © 2011 Wiley-VCH Verlag GmbH & Co. KGaA, Weinheim

Keywords: boron · glass ceramics · nanoparticles · salt melts

[1] B. Albert, H. Hillebrecht, *Angew. Chem.* **2009**, *121*, 8794 – 8824; *Angew. Chem. Int. Ed.* **2009**, *48*, 8640 – 8668.

[2] R. Penco, G. Grasso, *IEEE Trans. Appl. Supercond.* **2007**, *17*, 2291 – 2294.

[3] Q. Y. Zhang, J. Q. Xu, a. M. YZhao, X. H. Ji, S. P. Lau, *Adv. Funct. Mater.* **2009**, *19*, 742 – 747.

[4] M. Takeda, T. Fukuda, F. Domingo, T. Miura, *J. Solid State Chem.* **2004**, *177*, 471 – 475.

[5] N. Patel, R. Fernandes, G. Guella, A. Kale, A. Miotello, B. Patton, C. Zanchetta, *J. Phys. Chem. C* **2008**, *112*, 6968 – 6976.

[6] N. N. Greenwood, R. V. Parish, P. Thornton, *Q. Rev. Chem. Soc.* **1966**, *20*, 441 – 464.

[7] a) G. N. Glavee, K. J. Klabunde, C. M. Sorensen, G. C. Hadjapanayis, *Langmuir* **1992**, *8*, 771 – 773; b) C. Kapfenberger, K. Hofmann, B. Albert, *Solid State Sci.* **2003**, *5*, 925 – 930.

[8] a) T. T. Xu, J.-G. Zheng, A. W. Nicholls, S. Stankovich, R. D. Piner, R. S. Ruoff, *Nano Lett.* **2004**, *4*, 2051 – 2055; b) H. Zhang, Q. Zhang, J. Tang, L.-C. Qin, *J. Am. Chem. Soc.* **2005**, *127*, 8002 – 8003; c) Y. Li, E. Tevaarwerk, R. P. H. Chang, *Chem. Mater.* **2006**, *18*, 2552 – 2557; d) J. B. Levine, S. L. Nguyen, H. I. Rasool, J. A. Wright, S. E. Brown, R. B. Kaner, *J. Am. Chem. Soc.* **2008**, *130*, 16953 – 16958; e) P. Jash, A. W. Nicholls, R. S. Ruoff, M. Trenary, *Nano Lett.* **2008**, *8*, 3794 – 3798; f) G. Wang, J. R. Brewer, J. Y. Chan, D. R. Diercks, C. L. Cheung, *J. Phys. Chem. C* **2009**, *113*, 10446 – 10451; g) S. S. Amin, S.-y. Li, J. R. Roth, T. T. Xu, *Chem. Mater.* **2009**, *21*, 763 – 770.

[9] a) J. Ma, Y. Gu, L. Shi, L. Chen, Z. Yang, Y. Qian, *Chem. Phys. Lett.* **2003**, *381*, 194 – 198; b) L. Shi, Y. Gu, L. Chen, Z. Yang, J. Ma, Y. Qian, *Inorg. Chem. Commun.* **2004**, *7*, 192 – 194; c) Z. L. Schaefer, X. Ke, P. Schiffer, R. E. Schaak, *J. Phys. Chem. C* **2008**, *112*, 19846 – 19851; d) R. K. Selvan, I. Genish, I. Perelshtein, J. M. Calderon Moreno, A. Gedanken, *J. Phys. Chem. C* **2008**, *112*, 1795 – 1802; e) J. Ma, Y. Du, M. Wu, G. Li, Z. Feng, M. Guo, Y. Sun, W. Song, M. Lin, X. Guo, *J. Alloys Compd.* **2009**, *468*, 473 – 476; f) M. Zhang, X. Wang, X. Zhang, P. Wang, S. Xiong, L. Shi, Y. Qian, *J. Solid State Chem.* **2009**, *182*, 3098 – 3104.

[10] a) L. M. Liz-Marzán, P. Mulvaney, *J. Phys. Chem. B* **2003**, *107*, 7312 – 7326; b) D. J. Milliron, S. M. Hughes, Y. Cui, L. Manna, J. Li, L.-W. Wang, P. A. Alivisatos, *Nature* **2004**, *430*, 190 – 195; c) C. J. Murphy, A. M. Gole, S. E. Hunyadi, C. J. Orendorff, *Inorg. Chem.* **2006**, *45*, 7544 – 7554; d) D. Portehault, S. Cassaignon, E. Baudrin, J.-P. Jolivet, *Chem. Mater.* **2007**, *19*, 5410 – 5417; e) M. Niederberger, N. Pinna, *Metal Oxide Nanoparticles In Organic Solvents: Synthesis Formation, Assembly and Application*, Springer, Berlin, **2009**.

[11] D. Portehault, C. Giordano, C. Sanchez, M. Antonietti, *Chem. Mater.* **2010**, *22*, 2125 – 2131.

[12] M. J. Bojdys, S. A. Wohlgemuth, A. Thomas, M. Antonietti, *Macromolecules* **2010**, *43*, 6639 – 6645.

[13] A. L. Ivanovskii, I. R. Shein, N. I. Medvedeva, *Russ. Chem. Rev.* **2008**, *77*, 467.

[14] D. Chen, L. Cao, F. Huang, P. Imperia, Y.-B. Cheng, R. A. Caruso, *J. Am. Chem. Soc.* **2010**, *132*, 4438 – 4444.

[15] H. Maeda, T. Yoshikawa, K. Kusakabe, S. Morooka, *J. Alloys Compd.* **1994**, *215*, 127 – 134.

[16] V. K. La Mer, R. H. Dinegar, *J. Am. Chem. Soc.* **1950**, *72*, 4847 – 4854.

[17] E. Medvedev, A. Komarevskaya, *Glass Ceram.* **2007**, *64*, 42 – 46.

[18] S. Nagarajan, V. Raman, N. Rajendran, *Mater. Chem. Phys.* **2010**, *119*, 363 – 366.

[19] L. N. Kugai, T. N. Nazarchuk, *Powder Metall. Met. Ceram.* **1975**, *14*, 509 – 511.

[20] T. Mori in *Boron Rich Solids*, Springer, Dordrecht, **2011**, pp. 63 – 81.

[21] E. Barraud, S. Begin-Colin, G. Le Caer, O. Barres, F. Villieras, *Int. J. Nanotechnol.* **2008**, *5*, 649 – 659.

[22] M. Zhang, H. Wang, H. Wang, T. Cui, Y. Ma, *J. Phys. Chem. C* **2010**, *114*, 6722 – 6725.

[23] B. A. Kovenskaya, T. I. Serebryakova, *Powder Metall. Met. Ceram.* **1970**, *9*, 415 – 417.

[24] P. Jash, M. Trenary, *J. Phys. Conf. Ser.* **2009**, *176*, 012011.

 © 2011 Wiley-VCH Verlag GmbH & Co. KGaA, Weinheim